Available online at www.sciencedirect.com
ScienceDirect
International Journal of Sediment Research 28 (2013) 194-209
INTERNATIONAL JOURNAL OF SEDIMENT RESEARCH
www.elsevier.com/locate/ijsrc

Turbulence, suspension and downstream fining over a sand-gravel mixture bed

K. GHOSHAL[1], Rahul MAZUMDER[2], C. CHAKRABORTY[3] and B. S. MAZUMDER[3*]

Abstract

Flume experiments were carried out to study the turbulence and its impact on suspension and segregation of grain-sizes under unidirectional flow conditions over the sand-gravel mixture bed. The components of fluid velocity with fluctuations were measured vertically using 3-D Micro-acoustic Doppler velocimeter (ADV). The theoretical models for velocity and sediment suspension have been developed based on the concept of mixing length that includes the damping effect of turbulence due to sediment suspension in the flow over the sand-gravel mixture bed. Statistical analysis of segregation of grain-sizes along downstream of the bed has been performed using the principle of unsupervised learning or clustering problem. Exploratory data analysis suggests that there is a progressive downstream fining of sediment sizes with selective depositions of gravels, sand-gravels and sand materials along the stream, which may be segmented into three regions such as, the upstream, the transitional and the downstream respectively. This contribution is relevant to understand the direction of ancient rivers, the bed material character in the river form, sorting process and its role in controlling the sediment flux through landscape.

Key Words: Sand-gravel mixture, Flow velocity, ADV, Suspension concentration, Size-sorting, Clustering

1 Introduction

The study of sediment transport has received much attention to the researchers for a long time, but most of the experiments on sediment transport are confined to sand grain-size. The details of previous literatures on sediment-laden flow are to be found in Ghoshal (2005) and Mazumder and Ghoshal (2006). The effects of sand-gravel mixture on velocity and suspension concentration are not well understood. It hitherto remains unclear whether the bed roughness due to sand-gravel mixture is mostly responsible for mobility of the selective materials to pick up sediments into suspension and for downstream fining of bed material sizes will be investigated.

In order to elucidate the role of sand-gravel mixture, an attempt has been made to study the turbulence, the sediment suspension and the fining of grain-sizes along downstream direction over the sand-gravel mixture bed using the principle of unsupervised learning or statistical clustering technique which is not studied so far. The process of transportation due to turbulent flow over sand-gravel mixture bed is itself a complex phenomenon, because a proportion of sand materials is entrapped in the interstices of the coarse particles and removed from the bed surface; and on the other hand, sometimes coarse materials are entrapped by the fine sand particles during transportation (Parker et al., 1982; Iseya and Ikeda, 1987; Drake et al., 1988; Wilcock et al., 2001; Wilcock and Crowe, 2003; Mazumder et al., 2005a; Ghoshal et al., 2010). As such the accurate prediction of suspended materials is rather difficult, where the sediment bed is composed of sand-gravel mixture. Deigaard and Fredsoe (1978) investigated the longitudinal grain size sorting due to flowing water in alluvial channels, and observed that the mean grain size decreases in the downstream direction with the decrease of slope of the river. Experiments were designed, by Seal et al. (1997) in narrow-channels and by Toro-Escobar et al. (2000) in wide channels, to investigate the downstream fining materials through selective deposition of gravels which was achieved by feeding poorly sorted sediments at the upstream end of the flume and the evolution of the fining profile with time. Frostick et al. (2008) conducted series of flume experiments to study the effects of fine sand to the mobility of coarse materials, and they suggested that the presence of sand materials increased

[1] Assist., Prof., Department of Mathematics, Indian Institute of Technology, Kharagpur 721302, India. E-mail: koeli@maths.iitkgp.ernet.in
[2] Post-Doctoral Assoc., MIT, Cambridge, USA, E-mail: rahul.mazumder@gmail.com
[3] Prof., Fluvial Mechanics Laboratory, Physics and Earth Science Division, Indian Statistical Institute, Kolkata 700108, India, E-mail: chandan@isical.ac.in, and bijoy@isical.ac.in,
[*] Correspondence: E-mail: bijoy@isical.ac.in, Phone No. +91-33-2575 3033, Fax No. +91-33-25773026
Note: The original manuscript of this paper was received in June 2011. The revised version was received in Jan. 2013. Discussion opens until June 2014.

the mobility of gravels and led to a distinctive patchiness in bed break-up which supported the development of bedforms.

The objectives of the present study are to determine the turbulence and its impact on suspension and the progressive downstream fining of grain-sizes over the sand-gravel mixture bed. We propose a novel statistical clustering/ segmentation procedure, that splits the stream into three regions namely upstream, downstream and a transitional mid-stream by taking into account the averaged grain-size distribution. Though a general thinning of grain-sizes is observed, the problem of statistically quantifying the pattern of decrease of the grain-size and partitioning the length of the stream based on the strengths/nature of the grain sorting appeared to be unexplored. This research may have the contribution to understand the bed material character in the river form, sorting process and its role in controlling the sediment flux through landscape.

2 Experimental procedures

2.1 Experiments

Experiments were conducted in a closed circuit laboratory flume especially designed at the Fluvial Mechanics Laboratory (FML) of Indian Statistical Institute (ISI), Calcutta. A schematic diagram of the channel is provided in Fig. 1. The construction and operation had been discussed in Mazumder et al. (2005b). Both the experimental and the recirculating channels of the flume were exactly of the same dimensions (10m long × 50cm wide × 50cm high). Here the deposition of a part of sediment into the pipe of smaller cross section in commonly used flumes was avoided.

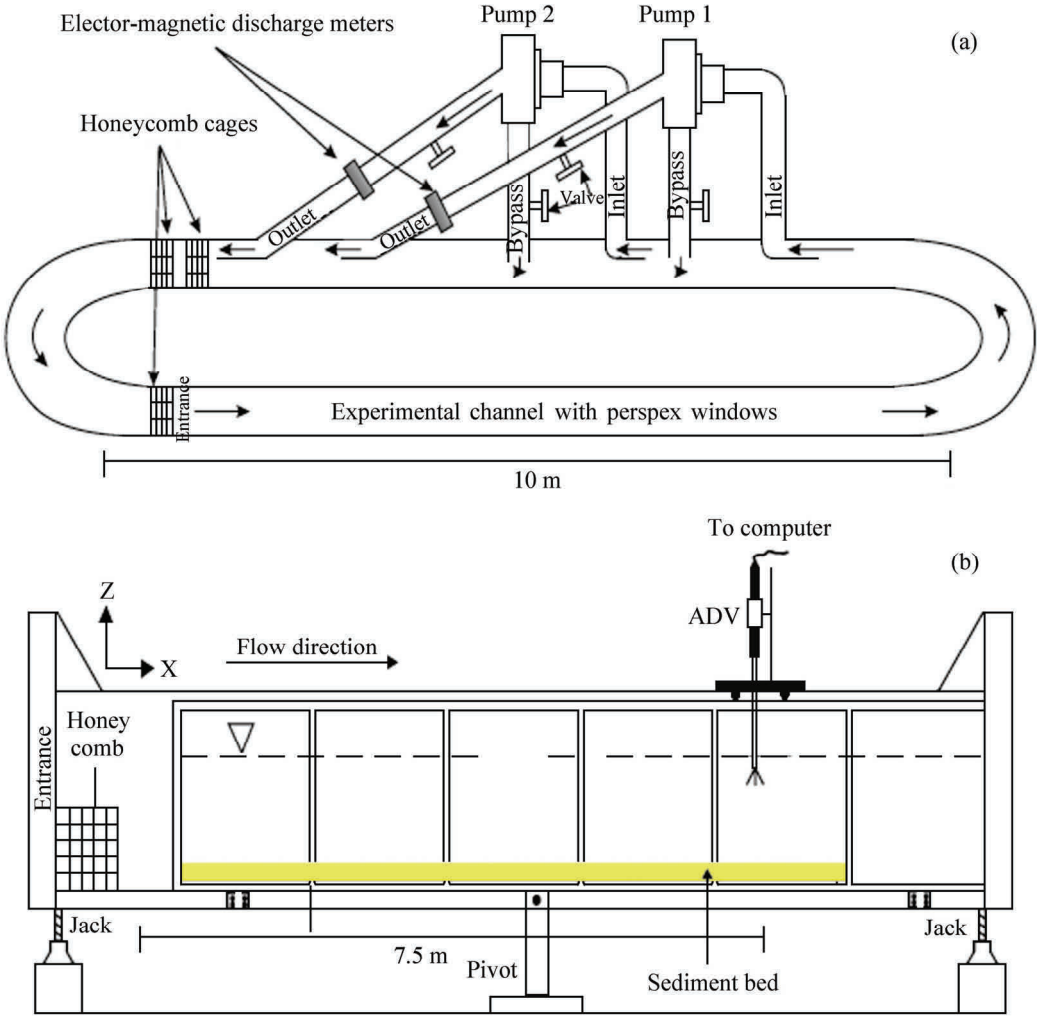

Fig. 1 Schematic diagram of the experimental channel. (a) Plan view, and (b) Front view

Generally, a part of sediment was used to remain hidden into the narrower recirculating pipe located below the experimental channel. The main advantage of the present flume was that the materials into the suspension came from the whole sediment bed moving throughout the flume without any lose of sediment from the bed materials. Two

electromagnetic discharge meters with digital display were fitted with the outlet pipes for continuous monitoring the water discharge. The upstream bend of the channel was divided into three sub-channels with equal dimensions and honey comb cages were placed at either end of sub-channels in order to ensure smooth, vortex free, uniform flow of water through the experimental channel.

Experiments were performed with a sediment bed of known grain-size distribution, consisted of heterogeneous mixture of sediment particles ranging from 0.032mm (5.0 phi) to 8mm (-3.0 phi), where phi = $-\log_2 D$ and D is the diameter of grain size in mm. The sediment bed used for the experiments had the peak value at 2.0 phi (0.25mm), and it was uni-modal distribution. Roughness value of the sediment bed was calculated by D_{65} (the sieve size of which 65% of the mixture by weight is finer) and the value of D_{65} was 1.65mm. The sediment bed was prepared by sand-gravel mixture in the proportion 25% gravel and 75% sand. The specific gravity of sediments used was 2.65. The cumulative-percentage plot of grain-size distribution of bed materials is shown in Fig. 2. The sediment mixture was laid down on the flume base to make a uniform plane bed of generally 3-4cm thick for the experiments. The water depth d was 30cm above the flume base. The experiment was initially started with a smooth and flat bed. The data collection procedures at the equilibrium bedforms and suspension above the bed were the same as that of earlier paper (Ghoshal et al., 2010, p. 2-3).

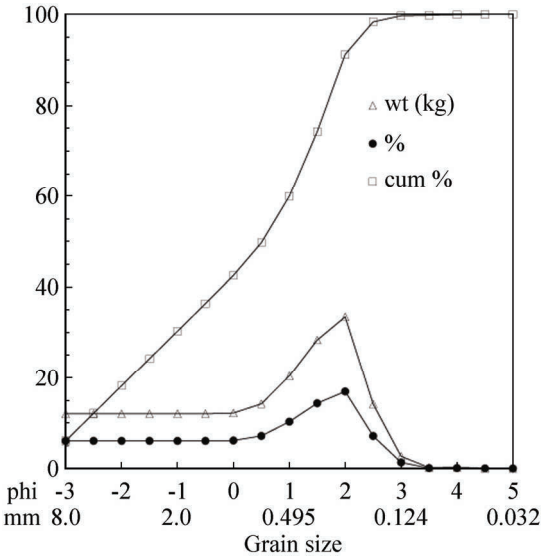

Fig. 2 Grain-size frequency distribution of the bed material

2.2 Velocity measurements

Velocity data with fluctuations were recorded at the mid-section of the channel using a SonTek 5cm down looking 3-D Micro-acoustic Doppler velocimeter (ADV) above the sediment bed for two different discharges ($Q \approx 0.135$ and $0.151 m^3 s^{-1}$). Hydraulic parameters are given in Table 1. The measurements were made along the vertical heights for five minutes at the sampling rate of 40 Hz to ensure full characterization of the flow. In order to assure the fully developed flow, the measuring section was chosen at a distance 7.5m downstream from source. The measuring locations were 5cm below the transmitter probe. The recorded data were free from the influence of the probe. The sampling volume was approximately cylindrical oriented along the transmitter beam axis. The size of the sampling volume for 16MHz ADV is 0.09 cm^3. The factory calibration of the ADV is specified to be 1% of the measured velocity. The ADV signals are affected by Doppler noise or white noise associated with the measurement process. The presence of this noise causes spikes in ADV signals. These spikes were removed by a phase space threshold despiking method described by Goring and Nikura (2002). The mean velocity profiles, turbulent intensities and shear stress were calculated from the filtered velocity data for two different maximum velocities (u_{max} = 95 and 105 cm s^{-1}) and the Froude Number F_r in the range of 0.57 to 0.65.

2.3 Bed load and suspension samples

After a sufficient time of run at each u_{max}, when the bedform and water slope were seemed to be steady state, and the materials in suspension were in equilibrium, samples of bedload and suspended load were collected with the help of siphon tubes (Ghoshal et al., 2010). Three repeated samples of suspended sediments with a fixed volume (5 lit) of sediment-laden water over a period of 15-16 minutes at the same height were collected simultaneously from the different heights of 5, 10, 15 and 20 cm above the sediment bed. Three bedload samples were also repeatedly siphoned from the top of the newly formed surface layer. It was obvious that the siphoning of bedload was somewhat hampered

due to the presence of gravels of size > 2mm in the sediment mixture ranging from 0.032 to 8 mm. The coarser grains at the bed surface did not move due to their weight. The smaller the grain with low settling velocity, the easier it is to move as bedload (Ghoshal et al., 2010). It was noticed that the transported materials were mostly the sand particles, and hence the downstream fining of selective sorting took place. After the removal of water, suspension and bedload samples were oven-dried. The amount of each size fraction was weighed by an electronic digital balance. The mean values of three repeated samples were analyzed. A record of bed conditions over the period of 15-16 minutes mentioned above was maintained and effective bed height (d') was obtained by averaging statistically the heights of bedforms and ripples recorded. While developing theoretical model for suspension concentration, it would be reasonable to use the effective bed height (d') because the influence of various moving bedforms was not effective in suspension when the system reached to a steady state (Mazumder et al., 2005a).

Table 1 Hydraulic parameters for experiments

Different Runs	Exp. 1 (Run 1)	Exp. 2 (Run 2)	Exp. 3 (Run 3)
Water discharge Q ($m^3 s^{-1}$)	0.135	0.151	0.175
Maximum mean velocity u_{max} (cm s^{-1})	95.00	105.00	116.00
Friction velocity u_* (cm s^{-1})	5.00	7.12	7.35
Slope (S)	0.001	0.002	0.0026
Water depth d (cm)	30	30	30
Bed roughness d_{65} (mm)	1.65	1.65	1.65
Bed thickness (cm)	3-4	3-4	3-4
Effective bed thickness d'(cm)	2.56	3.83	2.50
Effective water depth $H = d$-d' (cm)	27.44	26.17	27.50
Froude number F_r	0.57	0.65	0.71
Friction Reynolds number Re_*	15,000	21,360	22,050

2.4 Effective bed samples (EBS)

At the end of the experiments, when the suspended materials were fully deposited, the water was drained out carefully from the channel. In order to study the progressive downstream fining of grain-sizes during experiments, effective bed samples (EBS) were collected by scooping the approximate dimension of (3cm×3cm×3cm) from the top surface to the bottom, each 50cm apart from upstream to downstream up to 500cm. EBSs were collected for two independent experiments using two maximum velocity conditions ($Q \approx 0.151$ $m^3 s^{-1}$, $u_{max} = 105$ cm s^{-1}, $F_r = 0.65$ and $Q \approx 0.175$ $m^3 s^{-1}$, $u_{max} = 116$ cm s^{-1}, $F_r = 0.71$) from three locations across the width of the flume, namely the outer boundary, central and inner boundary. Here the EBSs across the width of the flume over the sediment bed were not collected for the discharge $Q \approx 0.135$ $m^3 s^{-1}$, ($u_{max} = 95$ cm s^{-1}, $F_r = 0.57$). The collected samples were oven-dried and sieved for 15 minutes at ½ phi interval by means of an electrically operated Ro-Tap sieve; and the amount of each sieve fraction was weighed by an electronic digital balance. From the data, one requires to understand the features in the grain size distribution that act as contrasts as one moves downstream.

2.5 Experimental observations

(u, v, w) and (u', v', w') denote respectively the time-averaged (mean) and the fluctuations of instantaneous velocity components (U,V,W) in the (x, y, z) directions, where x-axis along the flow, y-axis vertically upward and z-axis transverse to the flow. The vertical profiles of mean velocity components (u, v) illustrate the characteristic features of the flow over the sediment beds. The profiles of normalized stream-wise mean velocity u/u_* for two maximum velocities u_{max} = 95 and 105 cm s^{-1} are plotted against vertical co-ordinate ξ *(= y/H)* in Fig. 3(a, b), where u_* is the friction velocity determined from the log-law and $H = d - d'$ is the effective water depth. The stream-wise mean velocity profiles for both the flow conditions apparently exhibit a standard log-law with coefficient of regression R^2 as:

$$\frac{u}{u_*} = \frac{1}{\kappa} \ln \frac{y}{y_0} \tag{1}$$

where $\kappa = 0.4$ is the von Karman constant, y is measured from the sand bed surface, $y_0 \le y \le H$, and y_0 *(= k_s/30)* is the equivalent bed roughness determined from the log-law. Here u_* = 5.00 cm s^{-1}, y_0 = 0.0083 cm, slope of the bed surface $S = 0.001$ and $R^2 = 0.98$ for u_{max} = 95 cm s^{-1} and u_* = 7.12 cm s^{-1}, y_0 = 0.036 cm, $S = 0.002$ and $R^2 = 0.82$ for u_{max} = 105 cm s^{-1}.

The normalized vertical mean velocity v/u_* is plotted against vertical co-ordinate ξ *(= y/H)* in Fig. 4a for u_{max} = 95 cm s^{-1} and in Fig. 4b for u_{max} = 105 cm s^{-1}. It is interesting to note that the vertical mean velocity profiles show a parabolic type for both the flow conditions. Initially, the vertical velocity increases and reaches a maximum at a level about 30% of the depth and then decreases towards the free surface. In general, in the flat surface the vertical mean velocity profile shows zero value. Here the non-zero positive mean vertical velocity just above the moving sediment

bed exists due to the secondary circulation generated from the uneven bedforms. The vertical velocity distribution can be modelled by Beta density function, which collapses with the observed data, as

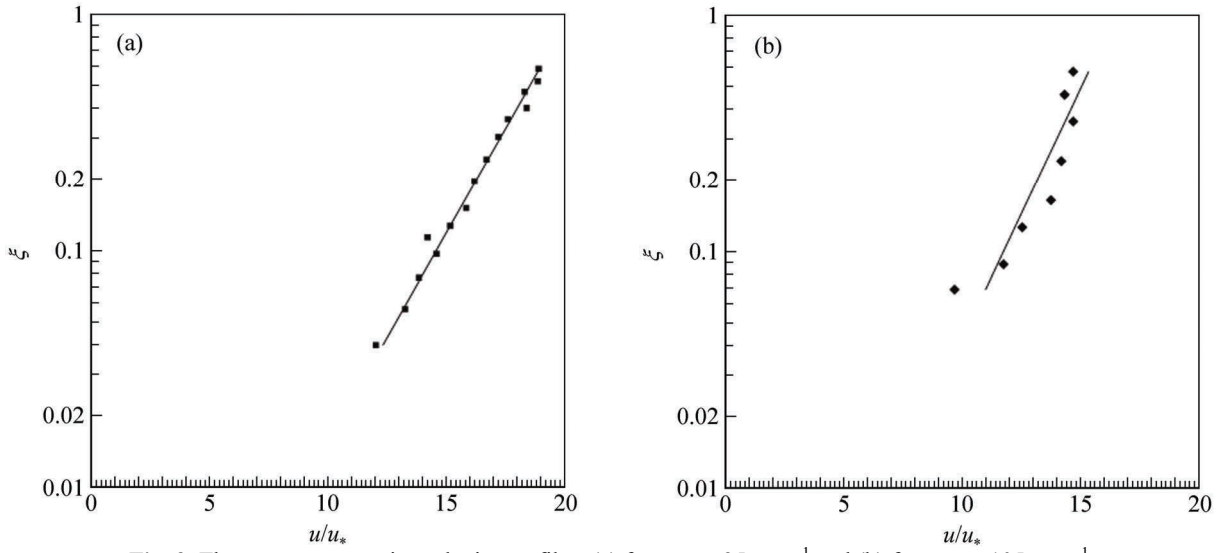

Fig. 3 The mean stream-wise velocity profiles: (a) for u_{max} = 95 cm s^{-1} and (b) for u_{max} = 105 cm s^{-1}

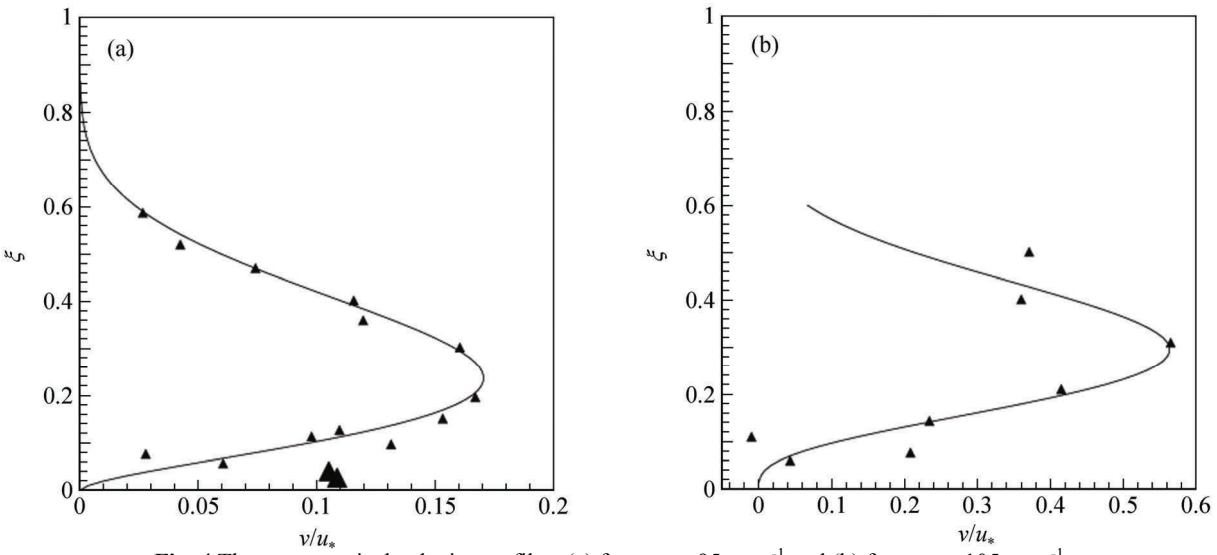

Fig. 4 The mean vertical velocity profiles: (a) for u_{max} = 95 cm s^{-1} and (b) for u_{max} = 105 cm s^{-1}

$$\frac{v}{b_0 u_*} = \frac{\Gamma(b_1 + b_2)}{\Gamma(b_1)\Gamma(b_2)} \xi^{(b_1 - 1)} (1 - \xi)^{b_2 - 1} \tag{2}$$

where b_1 and b_2 are the two positive shape parameters and b_0 is the scaling factor. These parameters are estimated from the observed data for different maximum velocities (u_{max}). Equation (2) agrees reasonably well for both the discharges and is shown in Fig. 4(a, b). Note that Eq. (2) upon division by the parameter b_0 is a Beta density function. The estimated parameters are b_0 = 0.063, b_1 = 2.7, b_2 = 6.5 with a coefficient of regression R^2 = 0.85 for u_{max} = 95 cm s^{-1}; and b_0 = 0.182, b_1 = 4.3, b_2 = 8.9 with R^2 = 0.71 for u_{max} = 105 cm s^{-1}. It may be noted that the velocity data collected by ADV near the bottom boundary showed a little irregular behavior due to erodible sediment bed (Fig. 4a), which were considered to be the outliers (bigger symbols).

Normalized stream-wise $\sigma_u (= \frac{\sqrt{\overline{u'^2}}}{u_*})$ and vertical $\sigma_v (= \frac{\sqrt{\overline{v'^2}}}{u_*})$ intensities of turbulence are respectively plotted in Fig. 5(a, b) and in Fig. 6(a, b) against vertical co-ordinate ξ *(= y/H)* for two maximum velocities u_{max} = 95 and 105 cm s^{-1}. Nezu and Rodi (1986) proposed the following empirical relations for σ_u, σ_v on the smooth rigid surface as

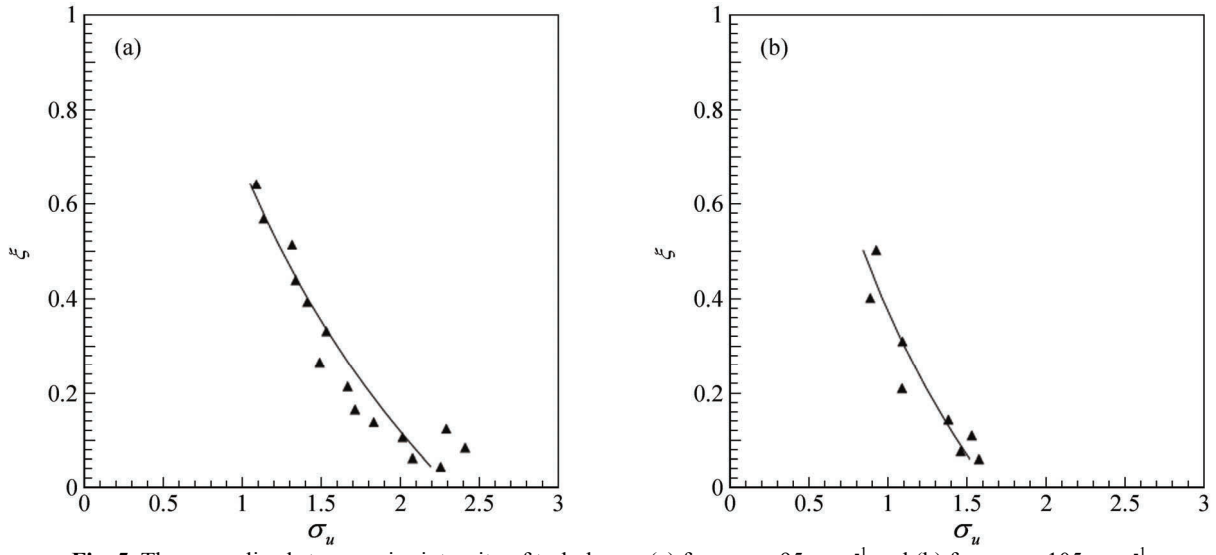

Fig. 5 The normalized stream-wise intensity of turbulence: (a) for u_{max} = 95 cm s^{-1} and (b) for u_{max} = 105 cm s^{-1}

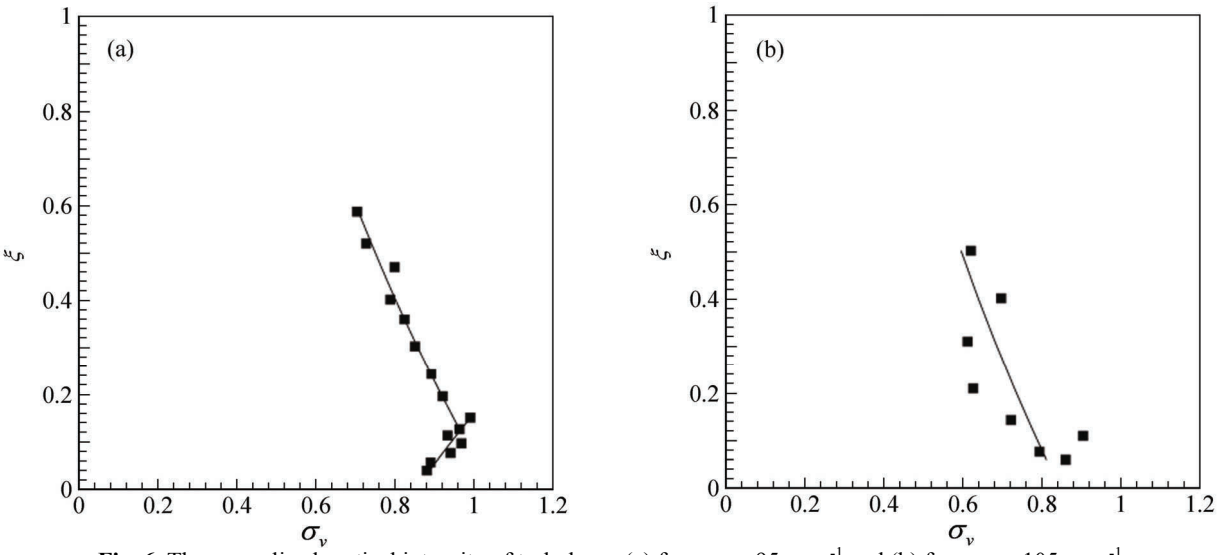

Fig. 6 The normalized vertical intensity of turbulence (a) for u_{max} = 95 cm s^{-1} and (b) for u_{max} = 105 cm s^{-1}

$$\sigma_u = D_u \exp\left(-\lambda_u \frac{y}{d}\right) \tag{3}$$

$$\sigma_v = D_v \exp\left(-\lambda_v \frac{y}{d}\right) \tag{4}$$

in which D_u, λ_u, D_v and λ_v are the empirical universal constants given by D_u = 2.26, λ_u = 0.88, D_v = 1.23 and λ_v = 0.67 respectively. It was observed that the above relations for both the intensities did not agree well with the observed data collected vertically over the erodible sediment bed. Therefore, the modified relations for σ_u and σ_v for two maximum velocities u_{max} = 95 and 105 cm s^{-1} over the moving sediment bed surface with values of R^2 were proposed as

$$\sigma_u = 2.31\exp(-1.24\xi), \quad R^2 = 0.91 \tag{5a}$$

$$\sigma_u = 1.64\exp(-1.34\xi), \quad R^2 = 0.89 \tag{5b}$$

and

$$\sigma_v = 0.71\exp(-0.99\xi), \quad 0 \le \xi \le 0.14, \quad R^2 = 0.96$$

$$= 0.87\exp(-0.67\xi), \quad 0.14 \le \xi \le 1.0, \quad R^2 = 0.81 \tag{6a}$$

$$\sigma_v = 0.70\exp(-0.70\xi), \quad R^2 = 0.56 \tag{6b}$$

which fitted well with the present data except σ_v for u_{max} = 105 cm s^{-1}. Only changes in coefficients of the formulations of turbulence intensities were visible for the flow conditions near the boundary generated due to the erodible beds. The values of D_u , λ_u , D_v and λ_v were estimated for two different runs.

The dimensionless mean Reynolds shear stress $\tau^+ (= -\overline{u'v'}/u_*^2)$ is shown against ξ in Fig. 7(a, b) for two maximum velocities (u_{max} = 95 and 105 cm s^{-1}). The normalized turbulent shear stress increases and reaches a maximum value at the level ξ = 0.14 near the bed and then decreases toward the free surface over the rough moving sediment beds. The qualitative behavior of shear stress agrees reasonably well with Nezu and Rodi (1986), but they did not provide any theoretical model to estimate the turbulent shear stress. Instead, an empirical model for the normalized shear stress was proposed by Lyn (1993) for open channel flow over the artificial dune covered surface as

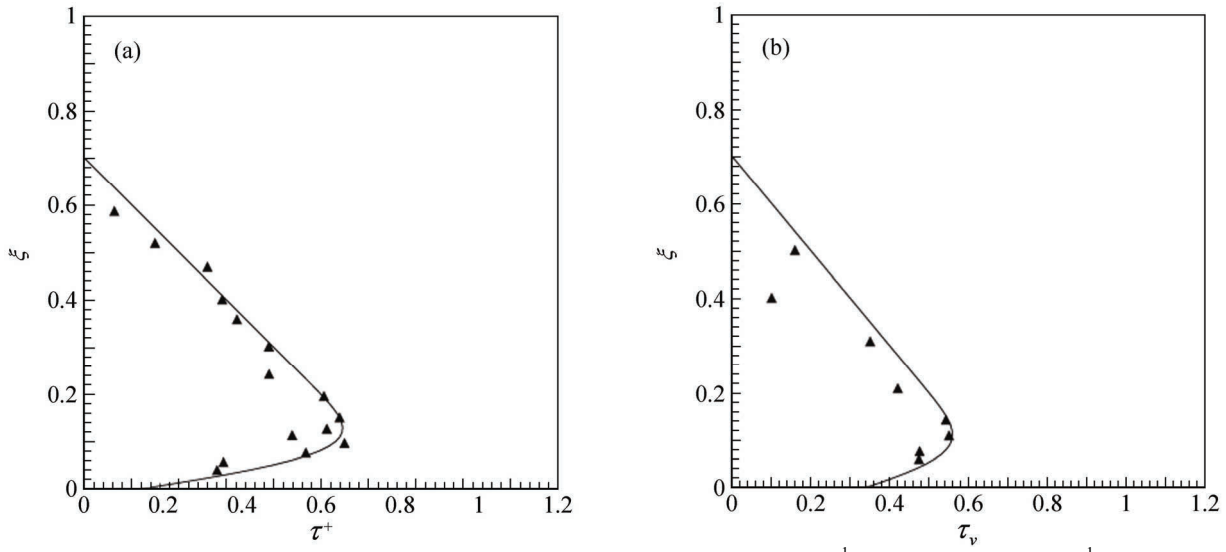

Fig. 7 Dimensionless mean Reynolds shear stress for: (a) u_{max} = 95 cm s^{-1} and (b) u_{max} = 105 cm s^{-1}

$$\tau^+ = (1 - \frac{y}{d}) - a_1 erfc\left[\frac{a_2 (y - d^+)}{d}\right] \tag{7}$$

where a_1 and a_2 are empirical constants determined from the test data and are given by 0.94 and 4.7; and d^+ is the elevation of the dune peak relative to the mean bed level. If a_1 = 0, Eq. (7) is identical to the linear shear stress expression that is conventionally used in open channel flow and the dimensionless shear stress goes to one as $y = 0$ for the flat surface. If $a_1 \neq 0$, the second term in Eq. (7) likely arises from the secondary circulation. Note that $a_1 > 0$ for downward flow which reduces the shear stress, and $a_1 < 0$ for upward flow leads to an increased shear stress.

However, for the flow over the loose sediment bed, measured turbulent mean shear stress τ^+ throughout the depth can be modeled as

$$\tau^+ = (1 - \xi - a_0) - a_1 erfc(a_2 \xi) \tag{8}$$

where a_1 and a_2 are parameters determined from the observed data along each vertical profile and a_0 is the scaling parameter. This equation agrees reasonably well through out the depth (Fig. 7a, b). The estimated parameters are given by a_0 = 0.3, a_1 = 0.58, a_2 = 11.0 with regression value R^2 = 0.81 for u_{max} = 95 cm s^{-1} and a_0 = 0.5, a_1 = 0.36, a_2 = 11.0 with R^2 = 0.74 for u_{max} = 105 cm s^{-1}. From Eq. (8) it is noticed that if a_1 = 0, Eq. (8) is an identical linear shear stress as conventionally used for open channel flow for the flat surface, but for the present case the mean shear stress τ^+ tends to the values 0.7 for u_{max} = 95 cm s^{-1} and 0.5 for u_{max} = 105 cm s^{-1} when ξ = 0 over the sediment bed surface.

The shear stress τ^+ from the Lyn's profile (7) shows the value as 0.06 at ξ = 0, and the value zero at ξ = 1, whereas the shear stress τ^+ from the present profile (8) shows the values as 0.12, 0.14 at ξ = 0, and the values -0.3, -0.5 at ξ = 1. Note that the value of τ^+ at ξ = 0 for the erodible beds (present case) is about two times of τ^+ at ξ = 0 at the rigid surface as indicated by Lyn (1993). For both the cases in Fig. 7(a, b), τ^+ is negative at the free surface indicating the counter clockwise rotation, which is presumably due to unevenness of the erodible sediment beds and it is zero below the free surface indicating the maximum velocity at that level.

3 Mathematical models

3.1 Velocity and suspension concentrations

In order to develop a theoretical model for velocity and suspension concentration, we consider two dimensional sediment-laden turbulent flow in an open channel with the origin of coordinates on the bed, where the *x*-axis along the flow and *y*-axis vertically perpendicular to the flow. When the turbulent flow carries sediments in suspension over the erodible sediment bed, the net fluid density ρ is related to the volume concentration of suspended sediment C by

$$\rho = \rho_f + (\rho_s - \rho_f)\, C = \rho_f\, [1 + AC] \tag{9}$$

where ρ_f is the density of clear fluid, ρ_s is the density of sediment and $A(= \rho_s / \rho_f - 1)$ is the relative density. The second term of (9) may be regarded as a perturbation to the density ρ_f of the clear water. The presence of density perturbation will inevitably change the flow characteristics; and hence the velocity should be the function of concentration. The turbulent shear stress τ_t due to Prandtl's momentum transfer theory is given by

$$\tau_t = \rho l^2 \left(\frac{du}{dy}\right)\left|\frac{du}{dy}\right| \tag{10}$$

where ρ is the net density of the fluid-sediment mixture, l is the mixing length and u is the mean velocity in the direction of flow. The total shear stress can also be represented as

$$\tau_t = \rho_f u_*^2 (1-\xi) \tag{11}$$

where $\xi = y/H$ and $H = d - d'$ is the effective water depth.

The form of mixing length l proposed by Kovacs (1998) is modified as

$$l = \left(0.4y - 0.44\frac{y^2}{H}\right)(1-C^{1/3}) \tag{12}$$

When $C = 0$, the Eq. (12) reduces to the mixing length $l = \left(0.4y - 0.44\frac{y^2}{H}\right)$ for clear water flow.

Using Eq. (12) for mixing length, the velocity gradient is as

$$\frac{du}{d\xi} = \frac{u_*(1-\xi)^{1/2}}{(0.4\xi - 0.44\xi^2)(1-C^{1/3})(1+AC)^{1/2}} \tag{13}$$

The momentum diffusion coefficient ε_m is given by

$$\varepsilon_m = \frac{\tau_t}{\rho_f (1+AC)\frac{du}{dy}} = (d-d')u_*(1-\xi)^{1/2}(0.4\xi - 0.44\xi^2)(1-C^{1/3})(1+AC)^{-1/2} \tag{14}$$

In a steady and uniform two-dimensional sediment-laden turbulent flow, where the concentration is constant in time and varies only with vertical coordinate y, the vertical distribution of suspension concentration C with particle settling velocity ω_s could be obtained as (Rouse, 1937)

$$\varepsilon_s \frac{dC}{dy} + \omega_s C = 0 \tag{15}$$

Using the Reynolds' analogy $\varepsilon_s = \gamma \varepsilon_m$, the expression of dimensionless concentration gradient becomes

$$\frac{dC}{d\xi} = \frac{-\omega_s C}{\gamma u_*(1-\xi)^{1/2}(0.4\xi - 0.44\xi^2)(1-C^{1/3})(1+AC)^{-1/2}} \tag{16}$$

where γ is the ratio of sediment diffusion coefficient to the momentum diffusion coefficient. Equations (13) and (16) are coupled and solutions of these equations give the desired vertical velocity and concentration profiles.

3.2 Bed layer level

In order to solve the Eqs. (13) and (16), we need to know the reference level (top of the bedload layer); and the velocity and concentration at that level. Flume experiments with approximately uniform grain size suggested that a value of *2D* (*D* is the diameter of the grains) for bed-layer height may be appropriate. But in natural alluvial channels with variable grain size, shape and packing density, the situation is more complicated and a representative grain size of the distribution has to be identified. The effective bed-layer height of the heterogeneous sediment mixture is commonly represented by the grain-size in the bed such as D_{65}, D_{80} or D_{90}. The use of grain-size larger than the median is justified by the fact that it takes into account the greater than proportional influence of larger particles on flow resistance (Leopold et al., 1964). In the present study, the effective bed-layer height (reference height) has been taken as $2D_{80}$, where D_{80} = 0.4cm, so that it is sufficient to cover the diameter of the maximum grain size (8mm) present in the bed.

3.3 Velocity at bed layer level

The empirical relation for the velocity of a sediment particle in the bed layer $2D_{65}$ is given by Engelund and Fredsoe (1976) as

$$u = \delta u_* \left[1 - 0.7\sqrt{(u_{*c}/u_*)} \right] \tag{17}$$

where the value of δ is 9.0 for sand and u_{*c} is the critical shear velocity corresponds to Shields' grain movement for particular grain-size. Here it is assumed that the migration velocity of sediment size at the top of the bed layer is approximately equal to the fluid velocity at that layer (Mazumder, 1994). In the present case, the value of δ is estimated as 3.65 to match the computed velocity u with the observed value at the level $2D_{80}$. Here the critical shear velocity u_{*c} of the size $2D_{80}$ is read from the Fig. 5 of Kuhnle (1993).

3.4 Concentration at bed layer level

An attempt was made to determine the bed layer concentration at the level $2D_{80}$ using different models (van Rijn, 1984; Zyserman and Fredsoe, 1994; and others), but none of them was sufficient to describe it properly. Therefore, as suggested by Ghoshal et al. (2010), the expression of reference concentration proposed by Smith and McLean (1977) was used since it was supported by field measurements. According to Smith and McLean (1977), the bed layer concentration C_{ξ_a} at the reference level $\xi_a = 2D_{80}$ is given by

$$C_{\xi_a} = \frac{\gamma_0 C_b S_*}{1 + \gamma_0 S_*} \tag{18}$$

where $S_* = u_*^2 / u_{*_c}^2 - 1$ is the normalized excess shear stress, which is determined from the dimensionless critical shear stress (Kuhnle, 1993) for the size $2D_{80}$; and C_b is the relative bed concentration (0.7 for the present case). The value of γ_0 was estimated as 0.0001, and the computation of (16) with this value of γ_0 showed well in agreement with the observed concentration.

3.5 Estimation of velocity and suspension concentration

In order to compute the vertical concentration distribution at different levels ξ, the fourth order Runge-Kutta method was adopted to solve the non-linear first order coupled differential Eqs. (13) and (16). The velocity and concentration at reference level $2D_{80}$ were determined from (17) and (18). The efficiency of mathematical model had been tested using the observed velocity and suspension concentration data for these two runs. While computing the vertical suspension concentration profiles at different heights, the ratio γ value (the ratio of sediment diffusion coefficient to the momentum diffusion coefficient) was adjusted for the best fit of concentration profiles with the observed data. The estimated value of γ was found 1.8 for moderate velocity 95 cm s^{-1} which pick up the fine sediment in suspension and the value γ was 2.5 for higher velocity 105 cm s^{-1}, which pick up coarser sediment in suspension (Mazumder and Ghoshal, 2006). The value of γ depends on velocity, suspension concentration and the bed conditions. The measured and computed mean velocity (u) and concentration (C) are plotted in Fig. 8 for u_{max} = 95 cm s^{-1} and in Fig. 9 for u_{max} = 105 cm s^{-1} and found that measured and computed values agree reasonably well. Here we have used the effective water depth H = d - d' from the sediment bed surface, where d is the water depth from the flume base, and d' is the effective bed height (averaging the heights of ripple crests passing during the collection of samples) ranging from 2.50-3.83cm.

4 Statistical analysis of segregation of grain-sizes along downstream

To study the segregation of grain-sizes along downstream, the effective bed samples (EBSs) collected from outer, central and inner regions across the channel width were analyzed for two independent experiments carried out for u_{max} = 105 cm s^{-1} and 116 cm s^{-1} (explained in section 2.4). All together fifty effective bed samples (EBS) from upstream to downstream were used for analysis of segregation. The EBSs across the sediment bed were not collected for u_{max} = 95 cm s^{-1}. Here the percentage plots of grain-size distributions of EBS from upstream to downstream are shown in Fig. 10 for outer, central and inner regions of the channel for u_{max} = 116 cm s^{-1} only. It is interesting to note that the concentration distributions gradually change to almost uni-modal through a process of size-sorting at the bed when sediments are transported from upstream (bottom of the figure) to downstream (top) even from a bed of bimodal distribution of sand-gravel mixture. It is well understood from the grain transportation and segregation that – there should be some significant change in the distribution of the grain sizes deposited in the bed from upstream to downstream. In addition, the patterns of grain sorting at the central part from upstream to downstream were different from that of boundaries of the channel. At high velocity, the whole sediment bed migrated downstream in the form of ripples, thereby exposing each grain to the flow. Because of their weight, the coarser grains or gravels available in the bed were not eroded that much. The smaller the grain with low settling velocity, the easier it was to move along the flow as bedload. Thus, the hindrance effects on sorting due to the presence of gravel beds were observed. Moreover,

since the velocity at the near-wall regions was less than that at the mid-section of the channel due to the side-wall frictional effects and the secondary circulations, the patterns of grain-size sorting in the boundaries were different from that of the central part of the channel.

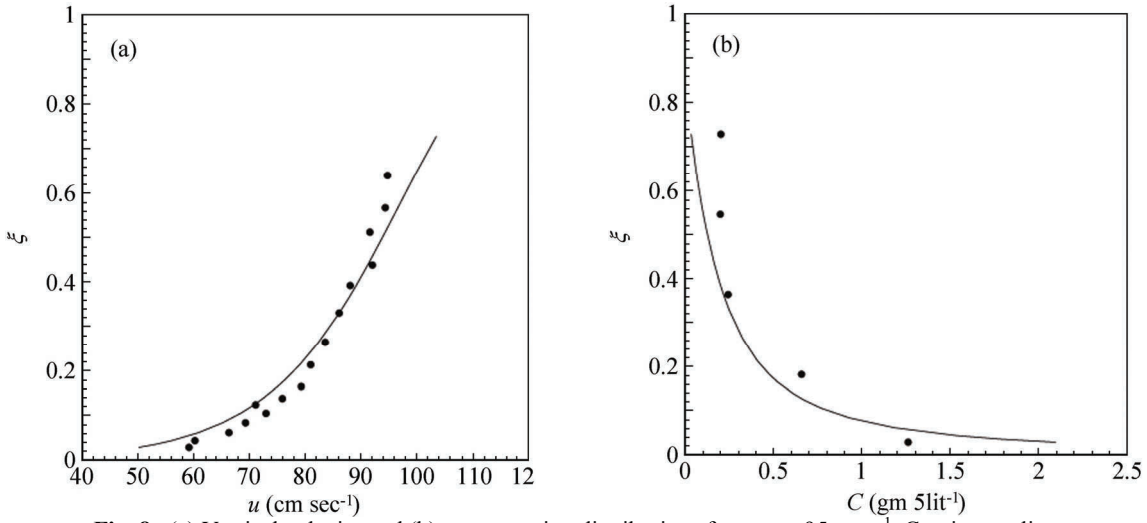

Fig. 8 (a) Vertical velocity and (b) concentration distributions for u_{max} = 95 cm s^{-1}. Continuous line and dots represent respectively the computed and the observed data.

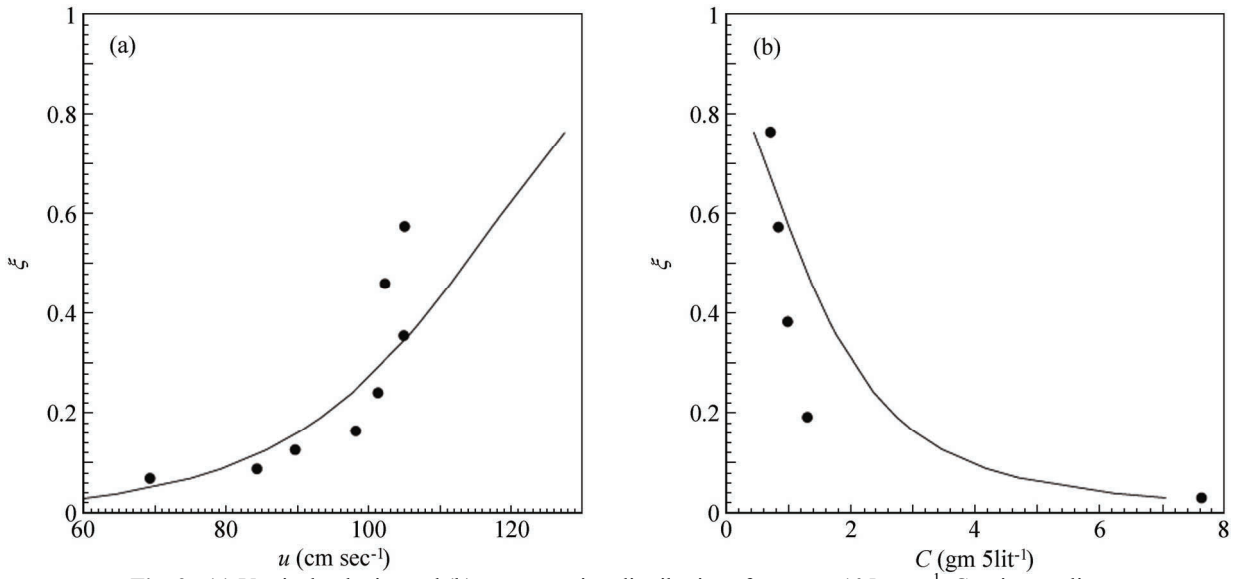

Fig. 9 (a) Vertical velocity and (b) concentration distributions for u_{max} = 105 cm s^{-1}. Continuous line and dots represent respectively the computed and the observed data.

It is a plausible assumption that certain features in the grain-size distribution vary along the length of the stream -- this variability partitions the stream into three parts. The partitioning, of course, is not arbitrary -- it should be such that the intra partition homogeneity (in the distribution of the grain-sizes) and inter partition heterogeneity (in the grain size distribution) are both maximized. We like to point out that this partition is not known a priori. Furthermore, even in presence of measurements corresponding to grain-size characteristics (across the length of the stream), partitioning is by no means a simple task. In this paper we like to carry out the partitioning via a disciplined statistical framework, without relying on ad-hoc ways of partitioning the stream.

Crisply stated the entire statistical analysis has the following two components:

1) First phase of analysis is the *Feature extraction,* which involves extracting features from the grain-size distribution corresponding to the different spatial locations along the stream, that seem to show characteristic and interesting variations across its length.

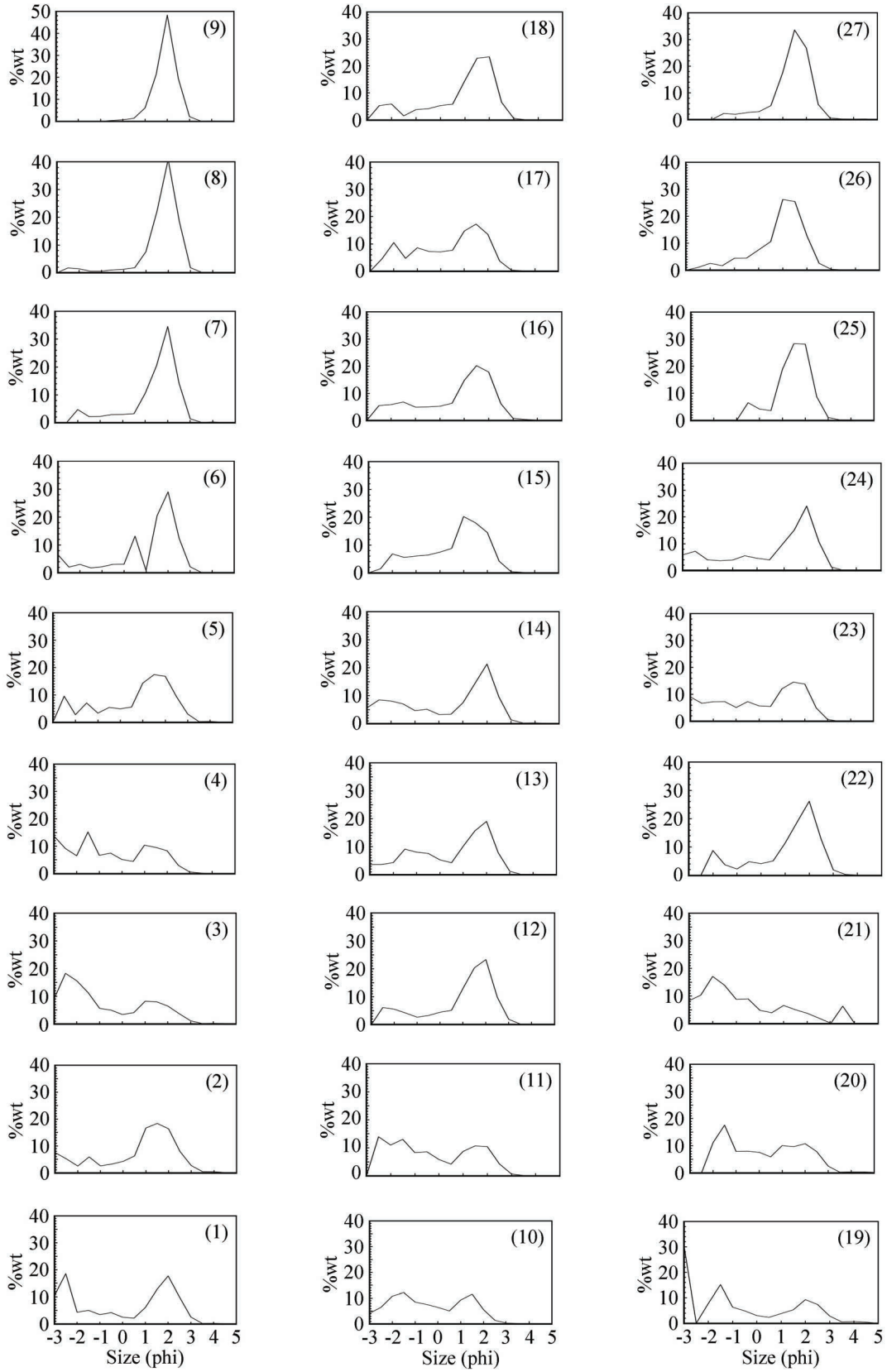

Fig. 10 Grain-size distributions of the effective bed samples from upstream (bottom of the figure) to downstream (top of the figure) for u_{max} = 116 cm s^{-1}. Distributions of first, second and third columns represent the outer, midsection and inner wall of the channel respectively. The horizontal axis represents the grain size (-3 phi to 5 phi) and the vertical axis represents the weight in percentage.

2) The second stage of the analysis is the *statistical clustering or segmentation* phase. Once the features are extracted, we employ statistical techniques to segment or partition the stream intro three parts with an eye towards maximizing both intra partition homogeneity and inter partition heterogeneity.

We have thus posed the problem as an unsupervised learning or statistical clustering problem (Hastie et al., 2001). Similar principles have been used in turbulence applications (Mazumder, 2007).

Exploratory data analysis suggested that the grain size distributions and certain statistics of the distributions, for example, mean, mode, among some others, show a visible change across the length of the stream. For the sake of interpretability we used the mean of the grain-size distribution as the feature to differentiate the location. This feature had been used in the segmentation algorithm for splitting the length of the stream into different parts.

4.1 Statistical segmentation: partitioning the stream

This section explores in detail the methods used for partitioning the length of the stream (from upstream to downstream) into different parts based on the distributional patterns of the grain-size concentration. We introduce a general framework for the basic statistical problem and propose a novel algorithm to obtain a solution for the same.

4.1.1 Motivation and formulation

Consider a general set-up where we have observations (ϕ_i, X_i), i = 1, . . . , m where ϕ_i is the scalar response variable (mean grain-size) and X_i the predictor variable (spatial locations, arranged in increasing order). Suppose there is a random time Λ, $\Lambda \in \{1,.....m\}$, such that, (ϕ_i, X_i), i = 1, . . . , Λ and (ϕ_i, X_i), i = Λ + 1, . . . , m come from different populations or clusters. While different types of modelling assumptions can be imposed on the populations, in what follows we will consider a more general situation where these different populations are characterized by flexible non-parametric regression models.

Suppose (ϕ_i, X_i), i = 1, . . . , n are realizations from an underlying functional relationship $X \mapsto \phi(X)$. In this application, the parametric form of $\phi(\cdot)$ is not known — so we propose to estimate $\phi(\cdot)$ via flexible non-parametric function estimation techniques (Silverman, 1986). One such non-parametric method is the local first degree least squares kernel estimator (Ruppert et al., 1995; Hastie et al., 2001) of the conditional mean $m(x) \equiv E(\varphi|X = x)$. This method proposes to estimate the functional value $\phi(x)$ at point $X = x$, via the conditional mean $m(x)$ using a kernel smoothing idea. The estimate is given by $\hat{\beta}_0$:

$$(\beta_0, \beta_1) = \arg\min_{\beta_0 \beta_1} \sum_{i=1}^{m} (\phi_i - \beta_0 - \beta_1 (X_i - x))^2 \times K((X_i - x)/h)/h \tag{19}$$

where h is the bandwidth, β_0 and β_1 are the regression coefficients, $K(u) = \exp(-\frac{1}{2}u^2)$ is the standard Gaussian kernel. The kernel K acts as a weight function, putting more weight on the data points X_i's close to $X = x$ and less weight on those far way from it — thereby giving a local flavour to the estimation procedure.

We will denote the local linear regression estimate at the point x at the bandwidth h, based on the observations (ϕ_i, X_i), $i = 1, \ldots, n$ by $\hat{m}(x; h; (\phi_i, X_i)_{i=1,\ldots,n})$.

The bandwidth h typically controls the degree of resolution with which the data is being viewed. A small choice of h will give an under smoothened estimate of the local mean $m(x)$ with revelation of features that are spurious sampling artifacts. Such an estimator has smaller bias and larger variance. A large value of h will give an over-smoothed version of the local mean, obscuring finer features — such an estimator has smaller variance and larger bias. There are theories that suggest choices for an optimal bandwidth, based on asymptotic bias variance trade-off (Ruppert et al., 1995). We will not pursue the approach of selecting an optimal bandwidth and hence doing the function estimation. We will pursue a different approach — that of Scale Space theory, the main idea of which is described as follows. This notion understands the object of interest (here properties of the local mean function) by assimilating information across different bandwidths instead of relying on a single 'optimal' bandwidth. This principle, which bypasses the problem of bias and variance associated with any particular estimate corresponding to a fixed bandwidth, is known in the computer vision literature as scale space (Chaudhuri and Marron, 1999; Leung et al., 2000). In this paper, we will understand certain characteristics, like the change points of the mean function by viewing it over a wide class of bandwidths. We will then assimilate the information acquired across variable bandwidths and solve the segmentation problem. Leung et al. (2000) addressed the issue of clustering via scale space methods in a different framework.

4.1.2 Algorithm description

It is believed that the behavioural characteristics of the segregation of grain sizes should be similar for the inner and outer boundaries of the channel and should differ from that of the central channel. Geologists' prior understanding of

the phenomenon of grain sorting suggests that the entire length of the stream (from upstream to downstream) should comprise typically of three segments — upstream, midstream and downstream. On more formal terms this means splitting (ϕ_i, X_i), $i = 1, \ldots, n$ into three disjoint segments — (ϕ_i, X_i), $i = 1, \ldots, \Lambda_1 - 1$; (ϕ_i, X_i), $i = \Lambda_1, \ldots, \Lambda_2 - 1$ and (ϕ_i, X_i), $i = \Lambda_2, \ldots, n$ for some Λ_1 and Λ_2 $(1 < \Lambda_1 < \Lambda_2 < n)$ such that (ϕ_i, X_i) values in each segment come from the same population and observations from different segments belong to different populations.

For λ_1 and λ_2 satisfying $(1 < \lambda_1 < \lambda_2 < n)$ obtain, $\hat{m}(x; h; (\varphi_i, X_i)_{i=1,\ldots,\lambda_1})$, $\hat{m}(x; h; (\phi_i, X_i)_{i=\lambda_1+1,\ldots,\lambda_2})$ and $\hat{m}(x; h; (\phi_i, X_i)_{i=\lambda_2+1,\ldots,n})$ as in Eq.(19). After that we determine the average residual sum of squares, for each of the three parts:

$$E_h(1, \lambda_1) = \frac{1}{\lambda_1} \sum_{j=1}^{\lambda_1} (\phi_j - \hat{m}(X_j; h; (\phi_i, X_i)_{i=1,\ldots,\lambda_1}))^2 \tag{20}$$

$$E_h(\lambda_1 + 1, \lambda_2) = \frac{1}{\lambda_2 - \lambda_1} \sum_{j=\lambda_1+1}^{\lambda_2} (\phi_j - \hat{m}(X_j; h; (\phi_i, X_i)_{i=\lambda_1+1,\ldots,\lambda_2}))^2 \tag{21}$$

$$E_h(\lambda_2 + 1, n) = \frac{1}{n - \lambda_2} \sum_{j=\lambda_2+1}^{n} (\phi_j - \hat{m}(X_j; h; (\phi_i, X_i)_{i=\lambda_2+1,\ldots,n}))^2 \tag{22}$$

These indicate the degree to which the function estimates agree with observed data.

For a fixed h, $(\Lambda_1(h), \Lambda_2(h))$ solves the following optimization problem:

$$\min_{(\lambda_1, \lambda_2),\, 1 < \lambda_1 < \lambda_2 < n} E_h(1, \lambda_1) + E_h(\lambda_1 + 1, \lambda_2) + E_h(\lambda_2 + 1, n) \tag{23}$$

and gives the optimal partition of the data space into three homogeneous populations. The segmentations depend upon the bandwidths. We combine these segmentations (indexed by h) together and come up with a robust choice of the three segments. Based on a equi-spaced grid (in the logarithmic scale) of the h values, namely $h_1, \ldots, h_J$, the two change points Λ_1 and Λ_2 are obtained as

$$\Lambda_i = median\,\{\Lambda_i(h_1), \ldots \Lambda_i(h_K)\},\ i = 1, 2. \tag{24}$$

To summarize the algorithm for the segmentation of a dataset (ϕ_i, X_i) $i = 1, \ldots, n$ into three segments characterized by two change points $1 < \Lambda_1 < \Lambda_2 < n$ is as follows:

Algorithm: Segment

1. Compute the local linear regression estimator $\hat{m}(x; h; (\phi_i, X_i)_{i=1,\ldots,n})$ for $x \in \{x_1, \ldots x_n\}$ for fixed h.

2. Compute the mean error of fits for the three parts $E_h(1, \lambda_1)$, $E_h(\lambda_1 + 1, \lambda_2)$ and $E_h(\lambda_2 + 1, n)$ *for* $1 < \lambda_1 < \lambda_2 < n$. Consequently evaluate $(\Lambda_1(h), \Lambda_2(h))$ (Eq. (23)).

3. Perform the above two steps for $h \in \{h_1, \ldots h_J\}$, a uniform grid on the logarithmic scale.

4. Obtain a robust estimate for the segmentation by averaging over the results obtained across different scales. In particular one may use Eq. (24).

4.1.3 Computation and results

As the sample size for each of the two experiments (u_{max} = 105 cm s^{-1} and 116 cm s^{-1}) is relatively small, we perform a synchronization of the two experimental data sets as per the downstream distance and form a larger pooled training/learning set. Our analysis is performed on the larger data-set for more meaningful statistical inference. We will use Segment for the midsection of the channel; and a combination of the inner and outer boundaries of the channel, and obtain partitions of the stream for the central, the inner and the outer channels.

Our learning data comprises of three samples $(\bar{\phi}_i^I, X_i^I), i = 1, \ldots n; (\bar{\phi}_i^C, X_i^C), i = 1, \ldots n$ and $(\bar{\phi}_i^O, X_i^O), i = 1, \ldots n$. Here $\bar{\phi}_i^I, \bar{\phi}_i^C, \bar{\phi}_i^O$ are the mean grain sizes at horizontal locations X_i^I, X_i^C, X_i^O (representing the distances from upstream), where superscripts correspond to the inner (I), central (C) and outer (O) channels respectively.

Segmentation of inner and outer boundaries

The inner and outer boundaries should ideally have a common upstream, mid-stream and downstream (Fig. 11a) for symmetry. All together thirty-three data points are used. For this purpose, the grain-size distribution of the two outer boundaries for two experiments (u_{max} = 105 cm s^{-1} and 116 cm s^{-1}) have to be considered simultaneously. For the inner and outer boundaries the common change points $(\Lambda_1^{I,O}(h), \Lambda_2^{I,O}(h))$ are solutions of the following optimization problem:

$$\min_{(\lambda_1, \lambda_2),\, 1 < \lambda_1 < \lambda_2 < n} (e_h^O(\lambda_1, \lambda_2) + e_h^I(\lambda_1, \lambda_2))$$

where

$$e_h^I(\lambda_1,\lambda_2) = E_h^I(1,\lambda_1) + E_h^I(\lambda_1+1,\lambda_2) + E_h^I(\lambda_2+1,n),$$
$$e_h^O(\lambda_1,\lambda_2) = E_h^O(1,\lambda_1) + E_h^O(\lambda_1+1,\lambda_2) + E_h^O(\lambda_2+1,n);$$

$E_h^I(1,\lambda_1), E_h^I(\lambda_1+1,\lambda_2), E_h^I(\lambda_2+1,n)$ and $E_h^O(1,\lambda_1), E_h^O(\lambda_1+1,\lambda_2), E_h^O(\lambda_2+1,n)$ are the averaged residuals (as in step 2 of Algorithm: Segment) obtained from the Inner (superscript *I*) and Outer (superscript *O*) channels respectively.

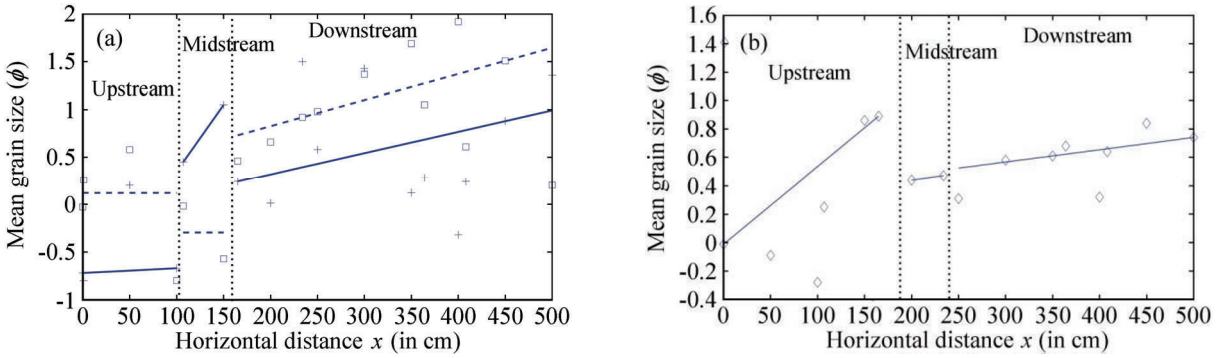

Fig. 11 (a) Segmentations and trend estimates for inner and outer boundaries of channel combining both the experiments (u_{max} = 105 cm s^{-1} and u_{max} = 116 cm s^{-1}). The `dashed' lines and `square' symbols represent respectively the computed and observed data from the outer boundary. The `solid' line and `plus' symbols represent respectively the computed and observed data from the inner boundary. All together thirty three observed data for outer and inner boundaries. (b) Segmentation and trend estimates for central part combining both the experiments (u_{max} = 105 cm s^{-1} and u_{max} = 116 cm s^{-1}). The `solid' lines and `diamond' symbols represent respectively the computed and observed data from the central part with seventeen observed data. Three segments namely upstream, midstream and downstream in the channel are shown.

Segmentation of the central channel

The partition of the central channel which is equivalent to the choice of $(\Lambda_1^C, \Lambda_2^C)$ is obtained by applying algorithm: Segment on the observations $(\bar{\phi}_i^C, X_i^C), i = 1,....n$ with J = 30. The segmentation corresponding to the choice of $(\Lambda_1^C, \Lambda_2^C)$ has been shown in Fig. 11b. Here all together seventeen data points collected from the central part of two experiments (u_{max} = 105 cm s^{-1} and 116 cm s^{-1}) are used for analysis. It is interesting to observe that the midstream basically acts as the transition between the upstream and downstream as is evident from its small stretch when compared to the upstream and downstream.

4.1.4 Estimation of trend

In the preceding section we described Algorithm Segment to obtain segmentations of the inner and outer boundaries of the channel, and the central channel. The algorithm is based on a flexible non-parametric non-linear estimation procedure – assuming no particular parametric form of the underlying function. The algorithm only gives the segmentation.

For the sake of easier interpretation and visualization, we would like to provide an estimate of the trend or pattern of decrease of the grain sizes as one moves from upstream to downstream. We will assume that the trend is linear for the sake of easier interpretation. This is obtained by solving a Constrained Least Absolute Deviation (CLAD) problem. This will provide three trend lines[1] for the three segments for each of the inner, central and outer of the channel.

The CLAD procedure for a data set $(\phi_i, X_i)_{i=1,...k}$ is given by the line $f(x) = \hat{a} + \hat{b}x$ where $(\hat{a}, \hat{b})$ solves the following convex optimization problem (Boyd and Vandenberghe, 2004)

$$\min_{a,b} \sum_{i=1}^{k} |\phi_i - a - bX_i|$$
such that $b \geq 0$

The constraint $b \geq 0$ is enforced because of the prior belief that the grain sizes are supposed to decrease with increasing distance from upstream. The ℓ_1 norm has been used, over the ℓ_2 norm to make the fit more robust to outliers / influential observations. The above procedure has been used to obtain trend estimates for each of the nine segments - three segments each for the inner, central and outer channels.

[1] unlike the case of segmentation, we allow the trend lines for the inner and outer channels to be different

5 Conclusions

The purpose of this study was to ascertain the role of heterogeneity of sand-gravel mixture to the mean flows, turbulence and suspension concentration; and to identify the stream of the channel. The principle of unsupervised learning or statistical clustering technique was used to analysis longitudinal fining of grain sizes at the erodible sand-gravel mixture bed during transportation.

The theoretical models for stream-wise velocity and suspension concentration have been developed based on the concept of mixing length, which is a function of concentration that contains the damping effect of turbulence in the flow. It is interesting to note that the non-zero vertical component of velocity generated due to the action of erodible sediment bed follows Beta density function.

From the experimental observations, it is noticed that a proportion of sand materials is entrapped in the interstices of the coarse particles and vice versa during transportation. However, for accurate estimation of suspension as well as active-layer concentration, a thorough laboratory study is required to understand the flow behavior and the grain-size fining process over the sand gravel mixture bed.

Statistical data analysis of longitudinal fining of grain sizes suggests a selective deposition along the length of the stream into three regions, such as, the upstream, the midstream and the downstream of the channel, considering the mean size of distributions along the bed as the feature of interest.

This research may have a significant contribution to infer the influence of heterogeneity of sand-gravel mixture in suspension as well as longitudinal fining of grain sizes during transportation. The motivation of this study is to understand the bed material character in the river form, sorting process and its role in controlling the sediment flux through landscape.

Acknowledgements

The authors would like to acknowledge the Department of Science and Technology (DST), New Delhi (Project No. SR/FTP/PS-67/2007) for their financial support to carry out this experimental research at the Indian Statistical Institute, Kolkata. The authors would like to thank two anonymous reviewers for their constructive comments and suggestions on the manuscript.

References

Boyd S. and Vandenberghe L. 2004, Convex Optimization, Cambridge University Press.

Chaudhuri P. and Marron J. S. 1999, Sizer for exploration of structures in curves. Journal of the American Statistical Association, Vol. 94, No. 447, pp. 807–823.

Deigaard R. and Fredsoe J. 1978, Longitudinal grain sorting by current in alluvial streams. Nordic Hydrology, Vol. 9, pp. 7–16.

Drake T. G., Shreve R. L., Dietrich W. E., Whiting P. J., and Leopold L. B. 1988, Bedload transport of fine gravel observed by motion-picture photography. Journal of Fluid Mechanics, Vol. 192, pp. 193–217.

Engelund F. and Fredsoe J. 1976, A sediment transport model for straight alluvial channels. Nordic Hydrology, Vol. 7, pp. 293–306.

Frostick L., Murphy B., and Middleton, R. 2008, Exploring the links between sediment character, bed material erosion and landscape: Implications from a laboratory study of gravels and sand-gravel mixtures. Geological Society, London, Special Publications, Vol. 296, pp. 117–127.

Ghoshal K. 2005, On velocity and suspension concentration in a sediment-laden flow: Experimental and theoretical studies. Ph. D. Thesis, Jadavpur University, Calcutta.

Ghoshal K., Mazumder B. S., and Purkait B. 2010, Grain-size distributions of bed load: Inference from flume experiments using heterogeneous sediment beds. Sedimentary Geology, Vol. 223, pp. 1–14.

Goring D. G. and Nikura V. I. 2002, Despiking acoustic Doppler velocimeter data. Journal of Hydraulic Engineering, Vol. 128, No. 1, pp. 117–126.

Hastie T., Tibshirani R., and Friedman J. 2001, Elements of Statistical Learning, Springer Verlag: N.Y.

Iseya F. and Ikeda H. 1987, Pulsations in bed load transport rates induced by a longitudinal sediment sorting: A flume study using sand and gravel mixtures. Geografiska Annaler, Vol. 69, No. 1, pp. 15–27.

Kovacs A. E. 1998, Prandtl's mixing length concept modified for equilibrium sediment-laden flows. Journal of Hydraulic Engineering, Vol. 124, No. 8, pp. 803–812.

Kuhnle R. A. 1993, Incipient motion of sand-gravel sediment mixtures. Journal of Hydraulic Engineering, Vol. 119, No. 12, pp. 1400–1415.

Leopold L. B., Wolman G, and Miller J. 1964, Fluvial processes in geomorphology. W. H. Freeman, San Francisco, California, USA.

Leung Y., Zhang J. S., and Xu Z. B. 2000, Clustering by scale space filtering. IEEE Transactions on Pattern Analysis and Machine Intelligence, Vol. 22, No. 12.

Lyn D. A. 1993, Turbulence measurements in open channel flows over artificial bedforms. Journal of Hydraulic Engineering, Vol. 119, No. 3, pp. 306–325.

Mazumder B. S. 1994, Grain size distribution in suspension from bed materials. Sedimentology, Vol. 41, pp. 271–277.

Mazumder R. 2007, Clustering based on geometry and interactions of turbulence bursting rate processes in a trough region. Environmetrics, Vol. 18, No. 4, pp. 445–459.

Mazumder B. S. and Ghoshal K. 2006, Velocity and concentration profiles in uniform sediment-laden flow. Applied Mathematical Modelling, Vol. 30, pp. 164–176.

Mazumder B. S., Ghoshal, K., and Dalal D. C. 2005a, Influence of bed roughness on sediment suspension: Experimental and theoretical studies. Journal of Hydraulic Research, Vol. 43, No. 3, pp. 245–257.
Mazumder B. S., Ray R. N., and Dalal D. C. 2005b, Size distributions of suspended particles in open-channel flow over sediment beds. Environmetrics, Vol. 16, pp. 149–165.
Nezu I. and Rodi W. 1986, Open-channel flow measurements with a Laser Doppler Anemometer. Journal of Hydraulic Engineering, Vol. 112, pp. 335–355.
Parker G., Klingeman P. C., and McLean D. G. 1982, Bedload and size distributions in paved gravel-bed streams. Journal of Hydraulic Division, ASCE, Vol. 108, No. 4, pp. 544–571.
Rouse H. 1937, Modern conceptions of the mechanics of fluid turbulence. Trans, ASCE, Vol. 102, pp. 463–543.
Ruppert D., Sheather S. J., and Wand M. P. 1995. An effective bandwidth selector for local least squares regression. Journal of the American Statistical Association. Vol. 90, No. 432, pp. 1257–1270.
Seal R., Paola C., Parker G., Southard, J.B., and Wilcock, P.R. 1997. Experiments on downstream fining of gravel: I. Narrow-channel runs. Journal of Hydraulic Engineering, Vol. 123, No. 10, pp. 874–884.
Silverman B. 1986, Density Estimation for Statistics and Data Analysis. Chapman and Hall: London.
Smith J. D. and Mclean S. R. 1977, Spatially averaged flow over a wavy surface. Journal of Geophysical Research, Vol.82, No. 12, pp. 1735–1746.
Toro-Escobar C. M., Paola C., Parker G., Wilcock P.R., and Southard J. B. 2000, Experiments on downstream fining of gravel: II. Wide and sandy runs. Journal of Hydraulic Engineering, Vol. 126, No. 3, pp. 198–208.
van Rijn L. C. 1984, Sediment transport, part II: Suspended load transport. Journal of Hydraulic Engineering, Vol. 110, No. 11, pp. 1613–1641.
Wilcock P. R. and Crowe J. C. 2003, Surface-based transport model of mixed-size sediment. Journal of Hydraulic Engineering, Vol. 129, No. 2, pp. 120–128.
Wilcock P. R., Kenworthy S. T., and Crowe J. C. 2001, Experimental study of the transport of mixed sand and gravel. Water Resources Research, Vol. 37, No. 12, pp. 3349–3358.
Zyserman J. A. and Fredsoe J. 1994, Data analysis of bed concentration of suspended sediment. Journal of Hydraulic Engineering, Vol. 120, No. 9, pp. 1021–1042.